Orbital design of formation flight to keep relative distance applied to space gravitational wave antenna B-DECIGO

Student Paper ☑

Shuhei Matsushita[1], Satoshi Ikari[1], Masaki Ando[2], and Shinichi Nakasuka[1]

[1] *Intelligent Space Systems Laboratory, Department of Aeronautics and Astronautics, The University of Tokyo, Tokyo, 113-8656, Japan*

[2] *Ando Laboratory, Department of Physics, The University of Tokyo, Tokyo, 113-8656, Japan*

Abstract

DECi-hertz Interferometer Gravitational wave Observatory, (DECIGO) is the planned Japanese space gravitational wave antenna. As precursor of DECIGO, B-DECIGO is also planned which will be consist of three formation flying satellites on Earth orbit. This gravitational wave antenna requires combined method of high-accuracy formation flight control and drag-free control which is advanced compensation system for observation of low gravitational wave. In the combined method, to keep relative position with noise reduction, spacecraft can adopt only low thrust power propulsion system such as 100 μN class thrusters. For formation flight orbit design in the constraint, this paper proposed an analytical method using the perturbation theory.

Keywords: Gravitational Wave Antenna, Formation Flight, Orbital Design, Record-disk orbit, Perturbation Theory

1. Nomenclature

a	=	semimajor axis, km
e	=	eccentricity
f	=	true anomaly
h	=	one of the non-singular orbital elements, $e\cos\omega$
I	=	angle of inclination to equatorial plane, rad
k	=	one of the non-singular orbital elements, $e\sin\omega$
L	=	distance, km
M	=	Mean anomaly, $\sigma + nt$, rad
$\hat{\boldsymbol{O}}$	=	coordinate
$\boldsymbol{p}$	=	orbital parameters to set a record-disk orbit, $\left(a_{ref}^{eci},\ I_{ref}^{eci}\ \Omega_{ref}^{eci},\ r_{sc},\ \Omega_{sc_1}^{ref},\ \sigma_{sc_1}^{ref}\right)$
P	=	amplitude of the time varying distance between spacecraft
r	=	distance from the center of the Earth, km
r_e	=	diameter of the Earth, km
r_{sc}	=	distance between spacecraft, km
R	=	perturbation function

t	=	time, s
$\hat{\boldsymbol{x}}, \hat{\boldsymbol{y}}, \hat{\boldsymbol{z}}$	=	unit vector
$\boldsymbol{x}$	=	(x, y, z), position of spacecraft
n	=	mean motion, rad/s
μ	=	gravitational constant, $\mathrm{km}^3/\mathrm{s}^2$
σ	=	epoch, rad
ϕ	=	initial separation angle between RAAN direction and spacecraft on circular orbit, $\omega + \sigma$, rad
ω	=	argument of perigee, rad
Ω	=	right ascention of ascending node (RAAN), rad
œ	=	orbital elements
$\bar{\text{œ}}$	=	non-singular orbital elements

Subscripts

$_e$	=	the Earth
$_{sc_N}$	=	spacecraft index $N = 1, 2, 3$
$_s$	=	the Sun
$_m$	=	the Moon
$_{ref}$	=	the orbital elements of reference circular orbit
$_{J_2}$	=	Geopotential J_2
$_{i,j,k,l}$	=	index of spacecraft

Superscripts

^{eci}	=	on ECI (Earth-Centered Inertial frame) $\hat{\boldsymbol{O}}^{eci}$
^{Hill}	=	on Hill's coordinate $\hat{\boldsymbol{O}}^{Hill}$
^{ref}	=	on reference orbit coordinate $\hat{\boldsymbol{O}}^{ref}$
^{sec}	=	secular
^{sp}	=	short-periodic

2. Introduction

2.1. Space Gravitational Wave Antenna : B-DECIGO [1]

On-ground gravitational wave(GW) observatories have already been examined and constructed, and the first direct detection of gravitational wave by aLIGO led gravitational wave astronomy to the next step [2]. However, due to distance limitation between interferometer mirrors and ground vibration, on-ground observatories target a frequency band of 10 Hz or higher and cannnot detect GW below 10 Hz. As means to detect lower frequency GW than ground observatories, space gravitational wave antenna where an interferometer can take the distance between mirrors more easily and is not influenced ground vibration is examined. Configuration of space gravitational wave antenna consists of three formation flying spacecraft in which the mirror constructing large interferometer.

The distance between the spacecraft is about $100 \sim 10^6$ km. To prevent the disturbance from the spacecraft applied to the mirror, the mirror is isolated from body of the spacecraft and controlled with only non-contact actuators. One of the space gravitational wave antenna, B-DECIGO(DECi-hertz Interferometer Gravitational wave Observatory) is being studied. *Fig. 1* This mission is precursor of DECIGO[1]. B-DECIGO targets GW frequency of $0.1 \sim 10$ Hz, which covers the gap between 100 Hz that ground GW observatories aim for and $10^{-3} \sim 10^{-2}$ Hz that space GW antenna LISA being examined by ESA[3] targets. Table.1 shows the specifications of B-DECIGO interferometer and Table.2 shows the requirements in B-DECIGO.

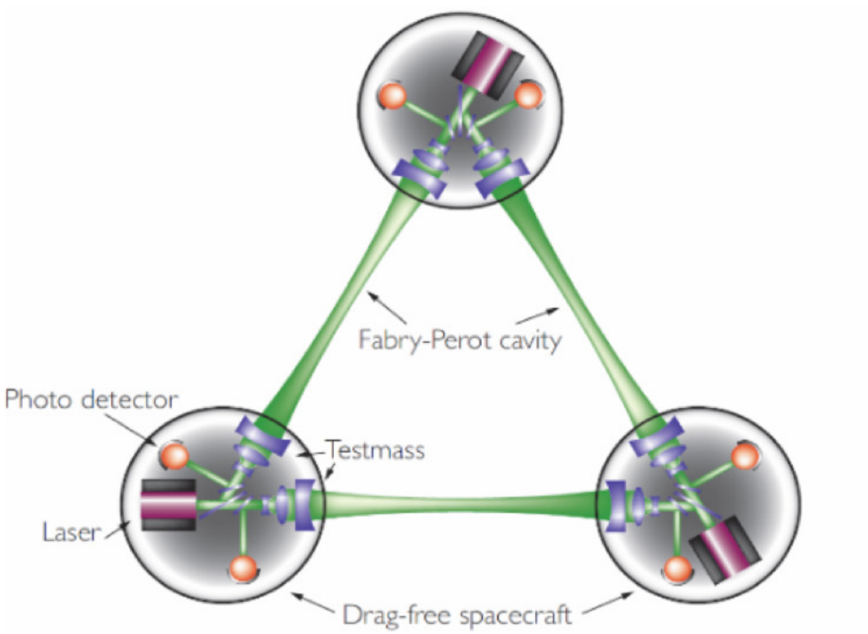

Fig. 1 B-DECIGO concept design [1]

Table 1 B-DECIGO Specifications

item	B-DECIGO
Distance between s/c	100 km
Effective Laser power	1 W
Laser wavelength	532 mm
Mass of mirror	30 kg
Diameter of mirror	30 cm

Table 2 B-DECIGO Requirements

item	requirements @0.1 Hz
Sensitivity	2×10^{-23} $/\sqrt{\text{Hz}}$
Acceleration noise per mirror	2×10^{-18} $\text{m}/\sqrt{\text{Hz}}$
Position Accuracy	±0.5%
Coupling	10^{-9} $/\sqrt{\text{Hz}}$
Noise to Mirror	7×10^{-19} $\text{m/s}^2/\sqrt{\text{Hz}}$
Noise to Spacecraft	3×10^{-10} $\text{m/s}^2/\sqrt{\text{Hz}}$

2.2. Requirements for Orbital Design

Requirements for orbital design in B-DECIGO are as follows,

1) stationary observation

2) keep the baseline length difference from other baseline lengths within ±0.5%
3) on Earth orbit

The requirement 2) means,

$$(1-0.5)\,L_{kl} < L_{ij} < (1+0.5)\,L_{kl} \tag{1}$$

In order to satisfy the requirement, the thrusters steadily used needs to satisfy 3×10^{-10} m/s^2/$\sqrt{\mathrm{Hz}}$(@0.1 Hz) of the noise requirement for spacecraft, and when the spacecraft weight is 600 kg, they must satisfy 2×10^{-7} N/$\sqrt{\mathrm{Hz}}$(@0.1 Hz). Thrusters satisfying this noise requirement have already been developed, such as cold gas jet thrusters, colloid thrusters, ion thrusters, and Field Emission Electric Propulsions(FEEPs). The maximum thrust of these thrusters satisfying the noise requirement is much smaller than a normal thruster, and it is about 100 μN. Therefore, the requirements for orbit design for stationary observation is formation flight orbit that can cancel the disturbance which changes the baseline length (the relative position of mirrors) with 100 μN thruster alone. The requirement 3) is for development of spacecraft. Since planned orbit of both LISA and DECIGO[1][3] are Sun orbit, their launch costs are higher than Earth orbit and downlink rate of mission data is limited. Therefore, B-DECIGO attempts to observe GW on Earth orbit, on which launch of spacecraft is easier and communication margin is more enough than Sun orbit. However, absolute disturbances on Earth orbit, mainly caused by the J_2, the Sun gravity and the Moon gravity, reach 10^{-5}m/s^2 order, which is much larger than maximum thrust of the micro thrusters. This means that using micro thrusters alone can't keep absolute orbit perturbed by these disturbances. Base on this, we aims to design an formation flight orbit on Earth orbit, on which three spacecraft can keep the distance between them to around 100 km satisfying the requiremnt 2), and make a control law with micro thruster to keep only relative position, without keeping absolute orbit.

Preliminary analysis for the orbital design and the control law construction, we analyzed how the J_2 disturbance affects on the distance between spacecraft by a numerical simulation and a theoretical analysis.

3. Record-disk orbit : keeping relative distance orbit

In order to keep relative distance between each spacecraft, we adopted record-disk orbit for B-DECIGO. This orbit is one of the solution of linearized relative equations: Hill equations [4], which show the relative motion of formation flying spacecraft in vicinity of virtual origin on reference circular orbit. This relative orbit is referred to as the general circular orbit (GCO), a cart orbit, or record-disk orbit [4][5].

In this paper, in order to express each spacecraft orbit in orbital elements, six orbital parameters $\boldsymbol{p} = \left(a^{eci}_{ref},\ I^{eci}_{ref}\ \Omega^{eci}_{ref},\ r_{sc},\ \Omega^{ref}_{sc_1},\ \sigma^{ref}_{sc_1}\right)$ is installed. a^{eci}_{ref}, I^{eci}_{ref} and Ω^{eci}_{ref} are semimajor axis, inclination, and right ascension of the ascending node (RAAN) of the reference circular orbit on ECI (Earth-Centered Inertial) frame $\hat{\boldsymbol{O}}^{eci}$ respectively. r_{sc} is the distance between spacecraft, in B-DECIGO mission this parameter is fixed, r_{sc} = 100km. $\Omega^{ref}_{sc_1}$ and $\sigma^{ref}_{sc_1}$ are RAAN and epoch of the first spacecraft on reference orbit coordinate $\hat{\boldsymbol{O}}^{ref}$. This coordinate is centered at the center of the Earth,the unit vector $\hat{\boldsymbol{x}}^{ref}$ is directed from the Earth's center to the right ascending node of reference circular orbit, $\hat{\boldsymbol{z}}^{ref}$ is normal to the reference circular orbit plane, and $\hat{\boldsymbol{y}}^{ref}$ completes the setup (see *Fig. 3*).

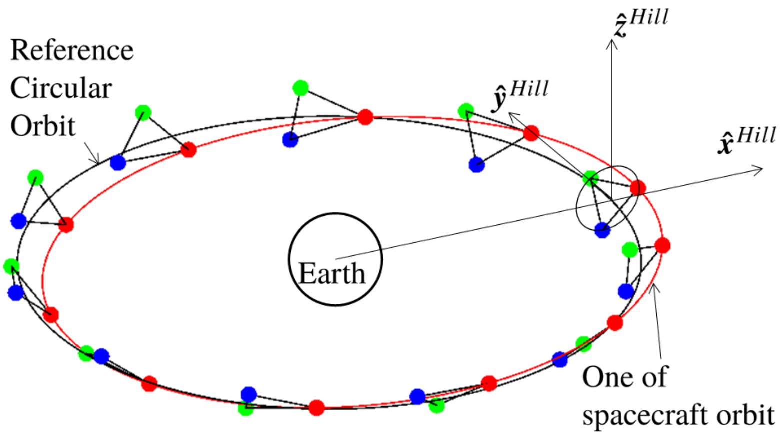

Fig. 2 Record-disk orbit [5]

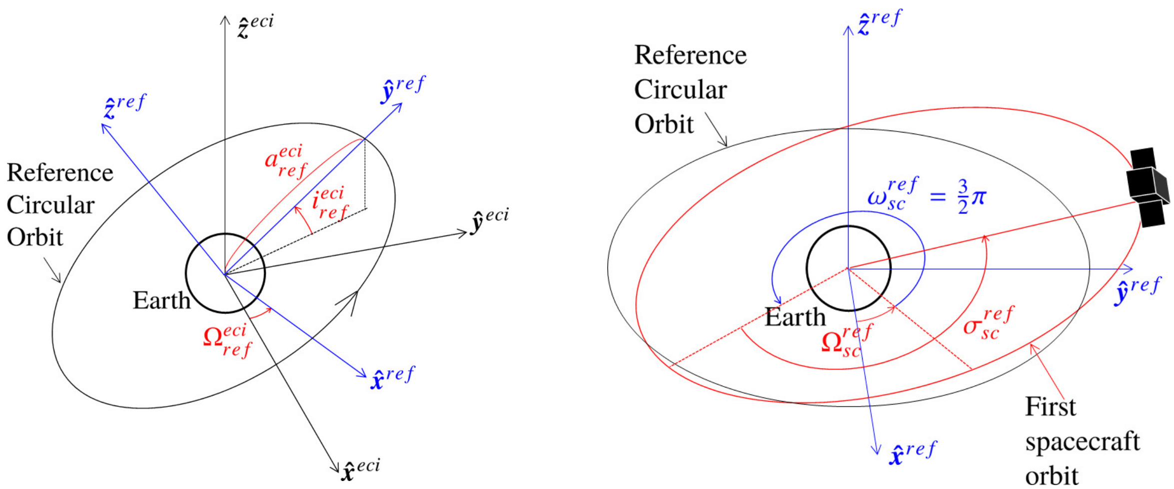

Fig. 3 Parameters and coordinates definition for expression of record-disk orbit

Each parameter has domain, $r_e \leq a^{eci}_{ref}$, $-\pi/2 \leq I^{eci}_{ref} \leq \pi/2$, $0 \leq \Omega^{eci}_{ref} \leq 2\pi$, $0 \leq \Omega^{ref}_{sc_1} \leq 2\pi/3$, and $0 \leq \sigma^{ref}_{sc_1} \leq 2\pi$. If $\Omega^{ref}_{sc_1}$, $\sigma^{ref}_{sc_1}$ are defined, RAAN and epoch on $\boldsymbol{O}^{ref}$ of other two spacecraft can be written as,

$$\begin{bmatrix} \Omega^{ref}_{sc_2} \\ \sigma^{ref}_{sc_2} \end{bmatrix} = \begin{bmatrix} \Omega^{ref}_{sc_1} + 2\pi/3 \\ \sigma^{ref}_{sc_1} - 2\pi/3 \end{bmatrix} \tag{2}$$

$$\begin{bmatrix} \Omega^{ref}_{sc_3} \\ \sigma^{ref}_{sc_3} \end{bmatrix} = \begin{bmatrix} \Omega^{ref}_{sc_1} + 4\pi/3 \\ \sigma^{ref}_{sc_1} - 4\pi/3 \end{bmatrix} \tag{3}$$

Using these parameters, orbital elements of each spacecraft $\mathbf{\oe}^{eci}_{sc_N} = \left(a^{eci}_{sc_N},\ e^{eci}_{sc_N},\ I^{eci}_{sc_N},\ \Omega^{eci}_{sc_N},\ \omega^{eci}_{sc_N},\ \sigma^{eci}_{sc_N}\right)$, $N = 1, 2, 3$ are obtained as following equations:

$$
\begin{aligned}
a^{eci}_{sc_N} &= a^{eci}_{ref} && (4)\\
e^{eci}_{sc_N} &= \frac{\sqrt{\left(a^{eci}_{ref} + \frac{1}{2}r_{sc}\right)^2 + \left(\frac{\sqrt{3}}{2}r_{sc}\right)^2}}{a^{eci}_{ref}} - 1 && (5)\\
I^{eci}_{sc_N} &= \arccos \frac{-C(N)}{\sqrt{A\,(N)^2 + B\,(N)^2 + C\,(N)^2}} && (6)\\
\Omega^{eci}_{sc_N} &= \begin{cases} \arctan \frac{A(N)}{B(N)} + \Omega^{eci}_{ref} & (B(N) \geq 0) \\ \arctan \frac{A(N)}{B(N)} + \pi + \Omega^{eci}_{ref} & (B(N) < 0) \end{cases} && (7)\\
\omega^{eci}_{sc_N} &= \begin{cases} \arccos \frac{\boldsymbol{\omega}^{eci}_{sc_N} \cdot \boldsymbol{\Omega}^{eci}_{sc_N}}{|\boldsymbol{\omega}^{eci}_{sc_N}||\boldsymbol{\Omega}^{eci}_{sc_N}|} & \left(C(N) \cdot \omega^{eci}_{3_{sc_N}} < 0\right) \\ \arccos \frac{\boldsymbol{\omega}^{eci}_{sc_N} \cdot \boldsymbol{\Omega}^{eci}_{sc_N}}{|\boldsymbol{\omega}^{eci}_{sc_N}||\boldsymbol{\Omega}^{eci}_{sc_N}|} + \pi & \left(C(N) \cdot \omega^{eci}_{3_{sc_N}} \geq 0\right) \end{cases} && (8)\\
\sigma^{eci}_{sc_N} &= \sigma^{ref}_{sc_N} && (9)
\end{aligned}
$$

here,

$$
\begin{aligned}
A(N) &= \frac{\sqrt{3}}{2} a^{eci}_{ref} r_{sc} \sin \Omega^{ref}_{sc_N} && (10)\\
B(N) &= \frac{\sqrt{3}}{2} a^{eci}_{ref} r_{sc} \cos \Omega^{ref}_{sc_N} \cos I^{eci}_{ref} + a^{eci}_{ref}\left(a^{eci}_{ref} + \frac{1}{2}r_{sc}\right) \sin I^{eci}_{ref} && (11)\\
C(N) &= \frac{\sqrt{3}}{2} a^{eci}_{ref} r_{sc} \cos \Omega^{ref}_{sc_N} \sin I^{eci}_{ref} - a^{eci}_{ref}\left(a^{eci}_{ref} + \frac{1}{2}r_{sc}\right) \cos I^{eci}_{ref} && (12)\\
& && (13)
\end{aligned}
$$

$$
\boldsymbol{\omega}^{eci}_{sc_N} = \begin{bmatrix} \left(a^{eci}_{ref} + \frac{1}{2}r_{sc}\right) \sin \Omega^{ref}_{sc_N} \\ -\left(a^{eci}_{ref} + \frac{1}{2}r_{sc}\right) \cos \Omega^{ref}_{sc_N} \cos I^{eci}_{ref} + \frac{\sqrt{3}}{2} r_{sc} \sin I^{eci}_{ref} \\ -\left(a^{eci}_{ref} + \frac{1}{2}r_{sc}\right) \cos \Omega^{ref}_{sc_N} \sin I^{eci}_{ref} - \frac{\sqrt{3}}{2} r_{sc} \cos I^{eci}_{ref} \end{bmatrix} = \begin{bmatrix} \omega^{eci}_{1sc_N} \\ \omega^{eci}_{2sc_N} \\ \omega^{eci}_{3sc_N} \end{bmatrix} \qquad (14)
$$

$$
\boldsymbol{\Omega}^{eci}_{sc_N} = \begin{bmatrix} B(N) \\ A(N) \\ 0 \end{bmatrix} \qquad (15)
$$

4. Numerical simulation

Firstly, numerical simulation was conducted to get directly how each spacecraft orbital parameter $\boldsymbol{p} = \left(a^{eci}_{ref},\ I^{eci}_{ref}\ \Omega^{eci}_{ref},\ r_{sc},\ \Omega^{ref}_{sc_1},\ \sigma^{ref}_{sc_1}\right)$ changes the observation time (time to deviate from requirement 2) Eq.(1)). Initial condition of each spacecraft is set by Eq.(4) ~ (9), disturbance is only J_2 geopotential. Orbital propagator is RK4, time-step is 10s. Using this simulator, we plotted the observation time in each orbital initial condition as grid search on $\left(I_{ref}^{eci},\ \Omega_{ref}^{eci}\right)$, and $\left(\Omega_{sc_1}^{ref},\ \sigma_{sc_1}^{ref}\right)$. On each grid search, other 4 parameters are fixed to proper value.

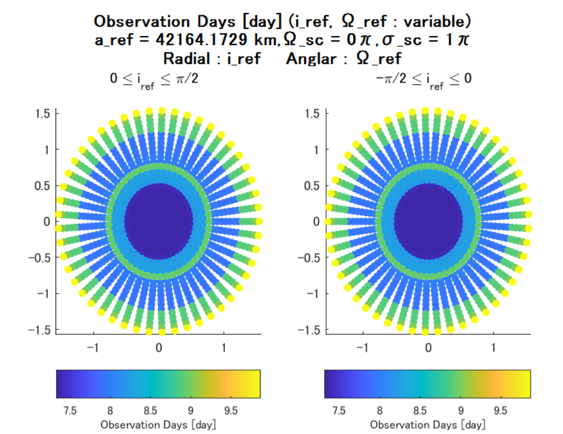

Fig. 4 *Grid search on* $\left(I_{ref}^{eci},\ \Omega_{ref}^{eci}\right)$

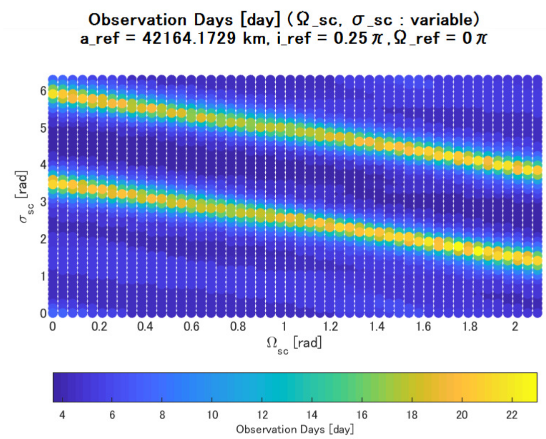

Fig. 5 *Grid search on* $\left(\Omega_{sc_1}^{ref},\ \sigma_{sc_1}^{ref}\right)$

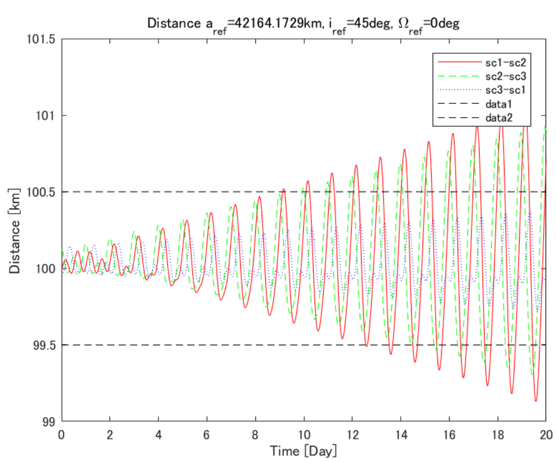

Fig. 6 *Time varying distance b/w spacecraft* L_{ij}

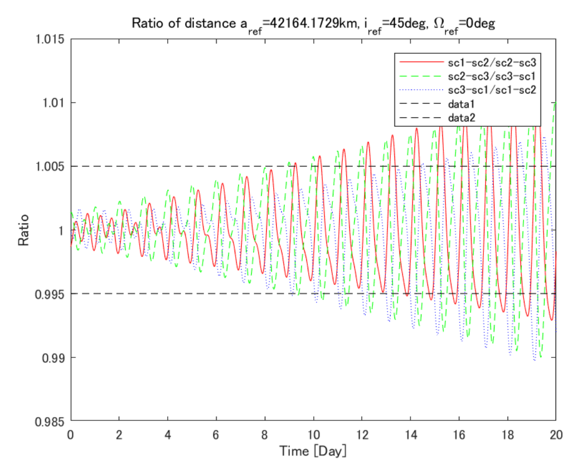

Fig. 7 *Time varying ratio of distance* L_{ij}/L_{kl}

Fig. 4 shows grid search result on $\left(I_{ref}^{eci},\ \Omega_{ref}^{eci}\right)$, and *Fig. 5* shows result on $\left(\Omega_{sc_1}^{ref},\ \sigma_{sc_1}^{ref}\right)$. *Fig. 4* also revealed observation days on each orbital condition don't depend on RAAN of reference orbit, Ω_{ref}^{eci}. Furthermore, *Fig. 5* revealed observation days is changed depending on $\Omega_{sc_1}^{ref} + \sigma_{sc_1}^{ref}$.

Then, *Fig. 6* shows time varying distance between spacecraft on one condition in *Fig. 4*. *Fig. 7* shows time varying ratio of distance L_{ij}/L_{kl} on same condition of *Fig. 6*. In this figure, black dotted lines shows the requirement 2), Eq. (1), so the time when any one reaches this dotted lines is defined as Observation days. *Fig. 8* shows DFT (discrete Fourier transformation) of the distance (*Fig. 6*)

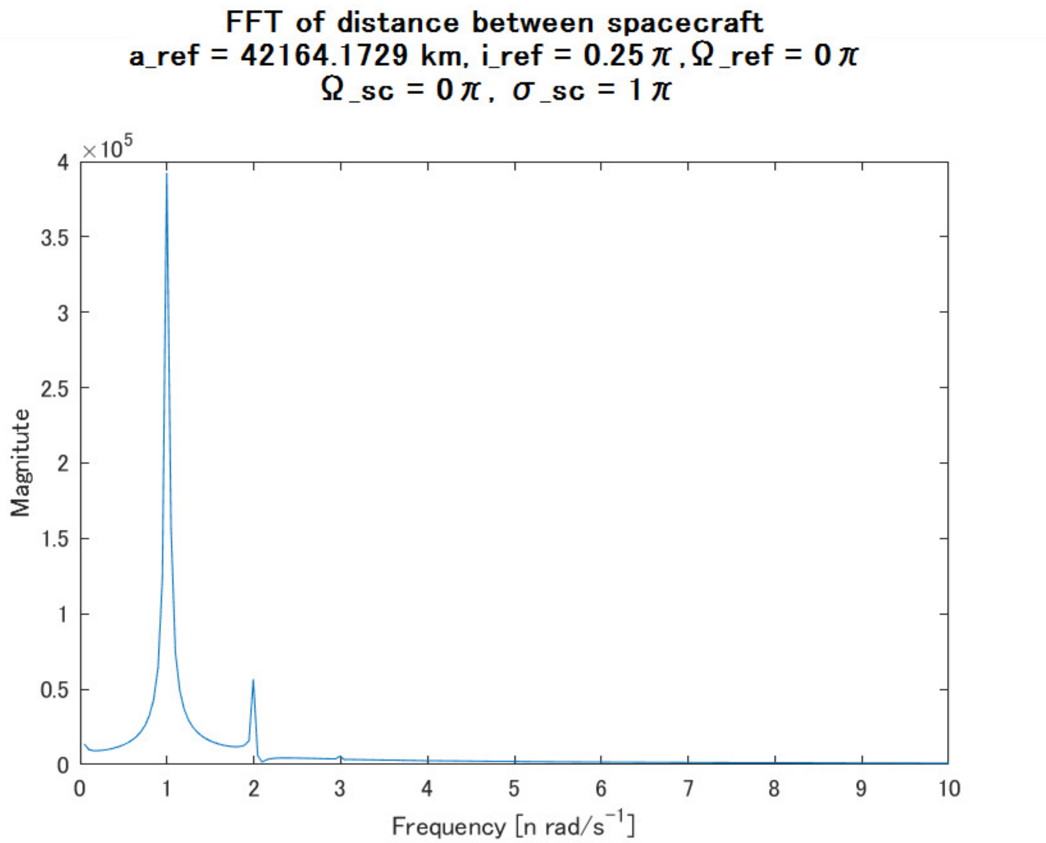

Fig. 8 DFT of distance between sc_1 and sc_2

and revealed that there are peaks on n_e and $2n_e$. This means the distance varying has mainly the same period as spacecraft orbit ($1/n_e$) and half period of it.

5. Analytical Method -Perturbation Theory-

5.1. Analytical expression of the distance between spacecraft

To reveal the disturbance causing the change of distance, we attempted to express the distance between spacecraft in only orbital elements. Hill et al., introduced below parameters in order to express the distance L_{ij} on orbital elements of each spacecraft[6].

$$\left(a_{sc_1}, e_{sc_1}, f_{sc_1}, a_{sc_2}, e_{sc_2}, f_{sc_2}, d, c_1, c_2\right)$$

$$L_{ij} = \sqrt{r_{sc_1}^2 + r_{sc_2}^2 - 2r_{sc_1}r_{sc_2}\left[\cos\left(c_1 - f_1\right)\cos\left(c_2 - f_2\right) + \sin\left(c_1 - f_1\right)\sin\left(c_2 - f_2\right)\cos d\right]} \quad (16)$$

In general, in kepler's orbital elements, i, Ω, ω can be defined differently depending on reference plane. Hill et al. set these parameters (d, c_1, c_2) not to depend on reference plane, therefore, we are able to substitute orbital elements of spacecraft on reference orbit plane $\boldsymbol{œ}^{ref}_{sc_N}$ to these three parameters. Furthermore, without perturbations, orbital elements of each record-disk orbit spacecraft on $\hat{\boldsymbol{O}}^{eci}$ are expressed as Eq. (4) ~ Eq. (9), and orbital elements on $\hat{\boldsymbol{O}}^{ref}$ are,

$$\begin{aligned} a^{eci}_{sc_N} &= a^{eci}_{ref} = a_{ref} & (17)\\ e^{eci}_{sc_N} &= e_{sc} \ll 1 & (18)\\ i^{ref}_{sc_N} &= \tan^{-1}\left(\frac{\frac{\sqrt{3}}{2}r_{sc}}{a^{eci}_{ref}+\frac{1}{2}r_{sc}}\right) & (19)\\ \Omega^{ref}_{sc_N} &= \Omega^{ref}_{sc_1} + \frac{2(N-1)}{3}\pi \quad (N=1,2,3) & (20)\\ \sigma^{ref}_{sc_N} &= \sigma^{ref}_{sc_1} - \frac{2(N-1)}{3}\pi \quad (N=1,2,3) & (21)\\ \omega^{ref}_{sc_N} &= \frac{3}{2}\pi & (22) \end{aligned}$$

Using these parameter on $\hat{\boldsymbol{O}}^{ref}$, with approximation $O(e^2) \simeq 0$ by Eq. (18), the square of the distance between spacecraft L^2_{ij} can be obtained,

$$\begin{aligned} L^2_{ij} \simeq\ & a^2_{ref}\ \left\{2-(1+\cos d)\sin\left(2c'-\frac{\pi}{3}\right)\right\}\\ &+ a^2_{ref}(1-\cos d)\cos\left(2M_{sc_1}-\frac{2}{3}\pi\right)\\ &+ a^2_{ref}e_{sc}\xi\sin\left(M_{sc_1}+\frac{\pi}{3}\right)\\ &+ a^2_{ref}e_{sc}(1-\cos d)\left(-2\cos^2 M_{sc_1}+\frac{3}{4}\cos M_{sc_1}-\frac{3\sqrt{3}}{4}\sin M_{sc_1}\right) \qquad (23) \end{aligned}$$

here,

$$\begin{aligned} \xi &= -(1+\cos d)\left\{\frac{5}{2}\cos 2c_1+\frac{3\sqrt{3}}{2}\sin 2c_1\right\}-2 & (24)\\ c' &= c_1+\frac{3}{2}\pi & (25) \end{aligned}$$

In this equation, Order of first term is $O(e^0)O((1-\cos d)^0)$, second term $O(e^0)O((1-\cos d)^1)$, third term $O(e^0)O((1-\cos d)^0)$, and fourth term $O(e^1)O((1-\cos d)^1)$. Since $\cos d \simeq 1$, $1-\cos d \ll 1$, $O(e^1)O((1-\cos d)^1) \ll O(e^1)O((1-\cos d)^0), O(e^1)O((1-\cos d)^1) \ll O(e^0)O((1-\cos d)^1)$. Therefore, fourth term $\simeq 0$.

First term is a constant, second term is time varying term with half period of orbit, $1/2n_e$, and third term is also time varying term with same period as orbit, $1/n_e$. These time varying term can be considered as compatible expression with the peaks in *Fig. 8*. Finally, in this paper, we evaluated the amplitude of these time varying term perturbed by J_2 term of geopotential, and compare with numerical simulation results.

5.2. Lagrange Planetary Equations

To evaluate the time differential of amplitude, we needs time differential of orbital elements perturbed by J_2 geopotential. For these expression, Lagrange's planetary equations on non-singular orbital elements are installed [7],

$$\frac{da}{dt} = \frac{2}{na}\frac{\partial R}{\partial \phi} \tag{26}$$

$$\frac{dI}{dt} = \frac{\cos I}{na^2\eta \sin I}\left(k\frac{\partial R}{\partial h} - h\frac{\partial R}{\partial k} + \frac{\partial R}{\partial \phi}\right) - \frac{1}{na^2\eta \sin I}\frac{\partial R}{\partial \Omega} \tag{27}$$

$$\frac{d\Omega}{dt} = \frac{1}{na^2\eta \sin I}\frac{\partial R}{\partial I} \tag{28}$$

$$\frac{dh}{dt} = -\frac{k\cos I}{na^2\eta \sin I}\frac{\partial R}{\partial I} + \frac{\eta}{na^2}\frac{\partial R}{\partial k} + \frac{h\eta}{na^2(1+\eta)}\frac{\partial R}{\partial \phi} \tag{29}$$

$$\frac{dk}{dt} = -\frac{h\cos I}{na^2\eta \sin I}\frac{\partial R}{\partial I} - \frac{\eta}{na^2}\frac{\partial R}{\partial h} + \frac{k\eta}{na^2(1+\eta)}\frac{\partial R}{\partial \phi} \tag{30}$$

$$\frac{d\phi}{dt} = -\frac{2}{na}\left(\frac{\partial R}{\partial a}\right) - \frac{\cos I}{na^2\eta \sin I}\frac{\partial R}{\partial I} + \frac{\eta}{na^2(1+\eta)}\left(h\frac{\partial R}{\partial h} + k\frac{\partial R}{\partial k}\right) \tag{31}$$

Since orbit of each spacecraft has small eccentricity, non-singular orbital elements $\bar{\mathbf{œ}} = (a, I, \Omega, h, k, \phi)$ should be used. These can be expressed by using Kepler's orbital elements as,

$$h = e\sin\omega,\ \ k = e\cos\omega,\ \ \phi = \omega + \sigma \tag{32}$$

5.3. Perturbation Function of J_2

Perturbation function of J_2 with approximation $O(e^2) \simeq 0$ can be written in the first order of (r_e/a) as,

$$R_{J_2} = \frac{\mu_e r_e^2}{a^3}J_2\left(1 + 3hS_\psi + 3kC_\psi\right)\left\{\left(\frac{3}{4}C_I^2 - \frac{1}{4}\right) + \frac{3}{4}S_I^2\left(C_{2\psi} + 4hS_{2\psi}C_\psi - 4kS_{2\psi}S_\psi\right)\right\} \tag{33}$$

here, $C_\theta = \cos\theta, S_\theta = \sin\theta$, and,

$$\begin{aligned}\psi &= \omega + M \\ &= \omega + \sigma + nt \quad (= \phi + nt)\end{aligned} \tag{34}$$

Substituting this perturbation function of J_2 to Eq. (26) ~ (31),

$$\frac{da}{dt} = \frac{nr_e^2}{a}J_2\left[-3S_I^2S_{2\psi}+\frac{3}{2}\left(3C_I^2-1\right)\left(hC_\psi-kS_\psi\right)+3S_I^2\left\{h\left(\frac{21}{4}C_{3\psi}+\frac{1}{4}C_\psi\right)-k\left(\frac{21}{4}C_{3\psi}-\frac{1}{4}C_\psi\right)\right\}\right] \tag{35}$$

$$\frac{dI}{dt} = -@@:\frac{3nr_e^2}{4a^2}J_2\sin 2I\sin 2\phi \tag{36}$$

$$\frac{d\Omega}{dt} = \frac{3nr_e^2}{4a^2}J_2\cos I\left(\cos 2\phi-2\right) \tag{37}$$

$$\frac{dh}{dt} = -\frac{3nr_e^2}{4a^2}J_2\left\{2k\cos^2 I\left(\cos 2\phi+1\right)+h\sin^2 I\sin 2\phi\right\} \tag{38}$$

$$\frac{dk}{dt} = -\frac{3nr_e^2}{4a^2}J_2\left(2h\cos^2 I\left(\cos 2\phi+1\right)+k\sin^2 I\sin 2\phi\right) \tag{39}$$

$$\frac{d\phi}{dt} = \frac{3nr_e^2}{2a^2}J_2\left\{\cos 2\phi\left(4\sin^2 I-1\right)+\left(4\cos^2 I-1\right)\right\} \tag{40}$$

5.4. Cost function

To evaluate the differential of distance between spacecraft, we introduced the time differential of the amplitude the third term P'_{12} in Eq.(23). In Eq.(23), $\xi = \xi\left(I_{sc_1}, I_{sc_2}, \Omega_{sc_1}, \Omega_{sc_2}, \omega_{sc_1}\right)$, and

$$P'_{12} = a_{ref}^2 e_{sc}\xi \tag{41}$$

Therefore, time differential of P'_{12} can be obtained as,

$$\frac{dP'_{12}}{dt} = 2\frac{da_{ref}}{dt}a_{ref}e_{sc}\xi+\frac{de_{sc}}{dt}a_{ref}^2\xi+\frac{d\xi}{dt}a_{ref}^2e_{sc} \tag{42}$$

Finally, we set the cost function for grid search evaluation as below,

$$J_{12} = \left|\frac{dP'_{12}}{dt}\right| \tag{43}$$

6. Evaluation of cost function

We compared the grid search result of numerical simulation and that of analytical cost function. If these two grid search are similar to each other, we were able to set proper cost function and ready to separate disturbances analytically.

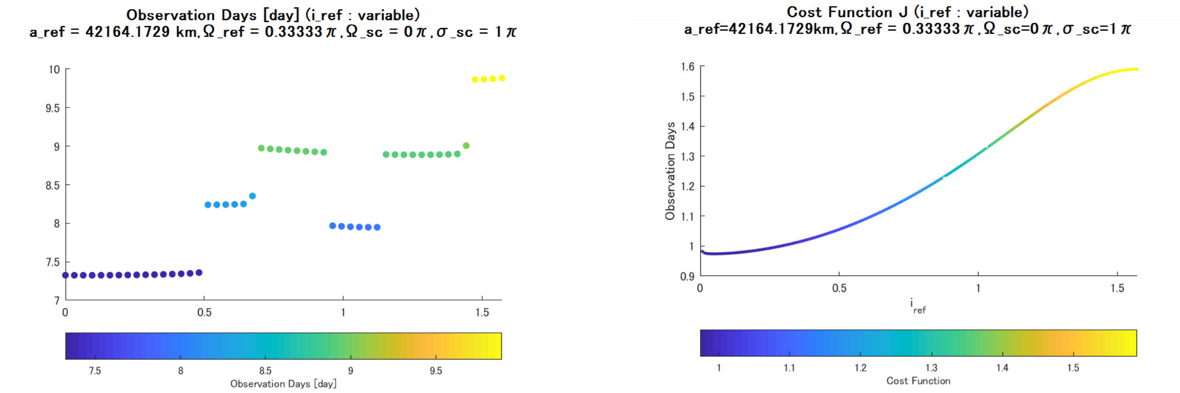

Numerical simulation result

Cost function analysis

Fig. 9 Grid search on I_{ref}^{eci}, $\left(\Omega_{sc}^{ref} = 0, \sigma_{sc}^{ref} = \pi\right)$

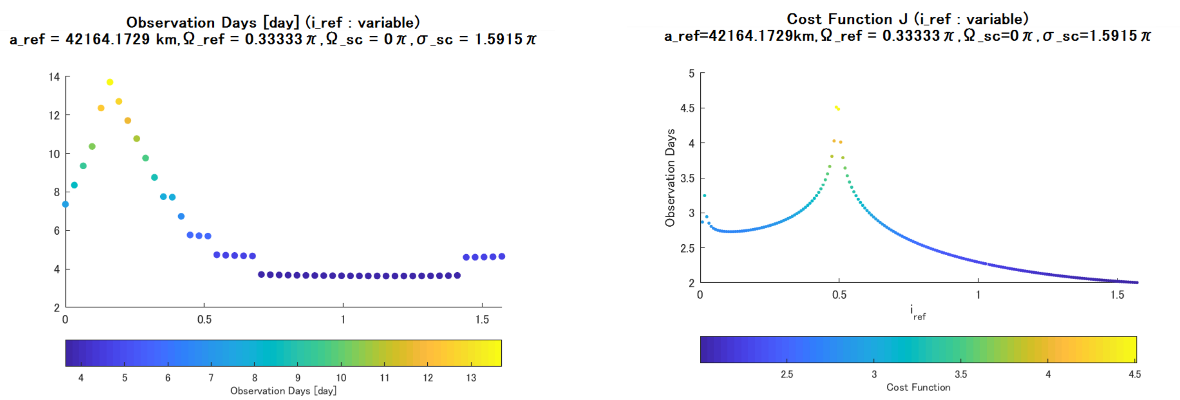

Numerical simulation result

Cost function analysis

Fig. 10 Grid search on I_{ref}^{eci}, $\left(\Omega_{sc}^{ref} = 0, \sigma_{sc}^{ref} = 5\right)$

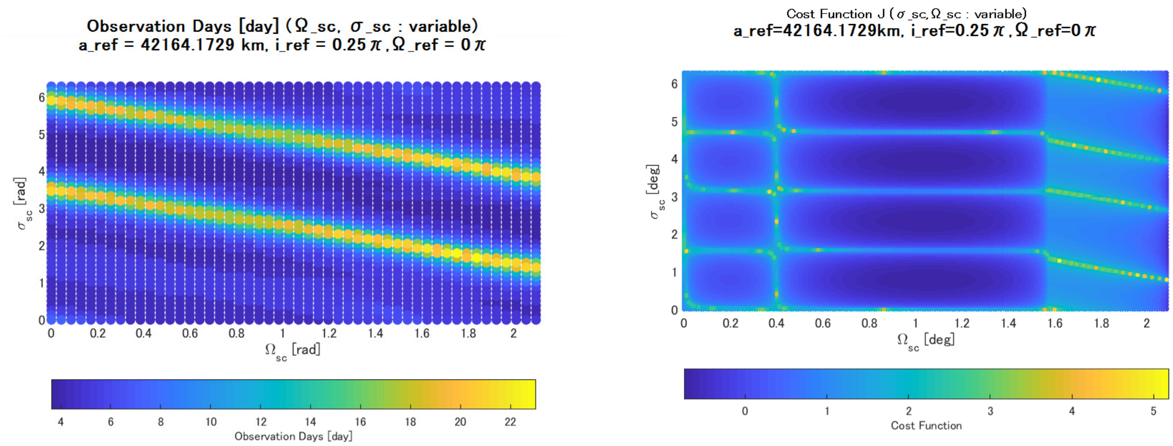

Numerical simulation result

Cost function analysis

Fig. 11 Grid search on $\left(\Omega_{sc_1}^{ref}, \sigma_{sc_1}^{ref}\right)$, $I_{ref}^{eci} = \pi/4$,

Fig. 9 show that the peak position and tendency of cost function analysis is similar to that of numerical simulation, However, in *Fig. 10*, the peak of cost function analysis is not match that of numerical simulation. On the other hand, in *Fig. 11*, at $\pi/2 < \Omega_{sc} < 2\pi/3$ the peak of cost function (thin color area) is very similar to the result of numerical simulation. At $\Omega_{sc} < \pi/2$, we should do more verification, but partially this cost function indicates the observation days, or the differential of the distance between spacecraft.

7. Conclusion

In this paper, in order to reach the requirements for B-DECIGO orbital design, the expression way of the time differential of the distance between spacecraft on record-disk orbit is presented. Then, installed perturbation theory on J_2 geopotential disturbance, the time varying distance between spacecraft is partially represented by the time differential non-singular orbital elements.

8. Future Work

Installed cost function represents theoretically the time-varying distance between spacecraft on record-disk orbit "without perturbed". However, considering the time differential of orbital elements perturbed by some disturbances makes it difficult to treat cost function in the same way. For instance, we focused only on the amplitude of the time varying distance, but actually the phase of the distance might be also changed. Therefore, we have to understand this expression of the distance more deeply. After that, the spacecraft thrusters control law will be constructed to reduce only the disturbance causing change of the distance between spacecraft.

References

[1] Kawamura, S., Nakamura, T., Ando, M., Seto, N., Tsubono, K., Numata, K., Takahashi, R., Nagano, S., Ishikawa, T., Musha, M., et al., "The Japanese space gravitational wave antenna-DECIGO," *Classical and Quantum Gravity*, Vol. 23, No. 8, 2006, p. S125.

[2] Abbott, B. P., Abbott, R., Abbott, T., Abernathy, M., Acernese, F., Ackley, K., Adams, C., Adams, T., Addesso, P., Adhikari, R., et al., "Observation of gravitational waves from a binary black hole merger," *Physical review letters*, Vol. 116, No. 6, 2016, p. 061102.

[3] Gath, P. F., Johann, U., Schulte, H. R., Weise, D., and Ayre, M., "LISA system design overview," *AIP conference proceedings*, Vol. 873, AIP, 2006, pp. 647–653.

[4] Alfriend, K. T., Vadali, S. R., Gurfil, P., How, J. P., and Breger, L. S., *Spacecraft formation flying: Dynamics, control and navigation*, Elsevier, 2009, Vol. 2.

[5] Kojima, H., Iwashima, H., and Trivailo, P. M., "Libration synchronization control of clustered electrodynamic tether system using kuramoto model," *Journal of Guidance, Control, and Dynamics*, Vol. 34, No. 3, 2011, pp. 706–718.

[6] Hill, K., and Born, G., "Autonomous interplanetary orbit determination using satellite-to-satellite tracking," *Journal of guidance, control, and dynamics*, Vol. 30, No. 3, 2007, pp. 679–686.

[7] Brumberg, V., *Essential relativistic celestial mechanics*, Routledge, 2017.